PHYSICAL REVIEW B VOLUME 36, NUMBER 5 15 AUGUST 1987-I

Molecular-dynamics computer simulation of amorphous molybdenum-germanium alloys

Kejian Ding and Hans C. Andersen
Department of Chemistry, Stanford University, Stanford, California 94305
(Received 20 January 1987)

A set of effective two-body and three-body empirical interatomic potentials are proposed for describing the short-range structure of amorphous alloys of molybdenum and germanium. Molecular-dynamics computer simulation calculations were performed for these alloys for a wide range of compositions with use of these potentials. The resulting structures have radial distribution functions, differential distribution functions, and partial distribution functions that are in very good agreement with recent x-ray scattering experiments of Kortright and Bienenstock for all the compositions studied. The experimental observation is confirmed that Mo atoms do not substitute into the germanium random network at low Mo concentrations. The calculations predict that at low concentrations the metal atoms tend to cluster together and that they significantly distort the random tetrahedral network of the germanium atoms in their vicinity.

I. INTRODUCTION

Most metal-metalloid glasses are prepared by rapid quenching of a liquid and can be prepared as amorphous materials only for a narrow range of concentration near a eutectic composition of about 20 at. % metalloid atoms. By means of vapor deposition, however, macroscopically homogeneous amorphous alloys of molybdenum and germanium can be prepared with compositions ranging from pure amorphous Ge to 65 at. % or even higher atomic fractions of Mo.[1] These alloys exhibit a rich variety of structures and electrical properties over this range of concentration.

The x-ray scattering experiments of Kortright and Bienenstock,[1,2] which included anomalous scattering as well as the usual radial distribution function (RDF) measurements, suggest that there are three structural regimes for these alloys. Region I ranges from 0 to less than 23 at. % Mo and is characterized by a gradual modification of the random tetrahedral network (RTN) of Ge by Mo atoms. Mo atoms do not substitutionally enter into the tetrahedral random network of Ge but modify the structure in their vicinity. The average nearest-neighbor coordination number is low (4–6). All the signs of tetrahedral *a*-Ge are not present a 23 at. % Mo. Region II, from 23 to 50 at. % Mo, shows a consistent local chemical ordering similar to that of Ge-rich intermetallic compounds. Region III, with greater than 50 at. % Mo, has the structural characteristics of the dense random packing of spheres, with higher coordination numbers (10–13).

An experimental study of the electrical properties of this system by Yoshizumi *et al.*[3,4] reveals that below 10 at. % Mo the system is a semiconductor and electron transport takes place by the mechanism of variable-range hopping. Above 10 at. % Mo the electrical properties are those of a typical metal. Accompanying the gradual structural modifications, the system undergoes two transitions as the atom fraction of molybdenum is increased: (1) from semiconductor to normal metal at about 10 at. % Mo; and (2) from normal metal to superconducting metal at about 13 at. % Mo.

A more complete understanding of the relationship of the structure and the electrical properties of these materials would clearly be worthwhile. Modern structural measurement techniques give useful but limited information relevant to understanding the structure of an amorphous material. The x-ray radial distribution function gives averaged information about the surroundings of all atoms as a function of distance. Anomalous x-ray scattering and x-ray absorption fine structure can in favorable cases give average information about the surroundings of the atoms of a specific atomic species. A more complete understanding of the structure must be based on a theoretical model that is consistent with the structural data.

A very promising way of constructing theoretical models for amorphous materials is to use molecular-dynamics (MD) computer simulations based on a choice of interatomic potentials. In this paper we report on the use of the data of Kortright and Bienenstock to develop interatomic potentials for the molybdenum-germanium system and a molecular-dynamics model of the structure of the amorphous alloys as a function of composition. Interatomic potential functions are the primary physical input to molecular-dynamics calculations. Our goal was to construct a set of empirical potential functions that were as simple as possible and that would account for the structures of the materials reasonably well.

In the following, we discuss molecular-dynamics computer simulation studies of the structures of amorphous molybdenum-germanium alloys using a set of empirical potential functions. Section II is devoted to the construction of the potential models. The molecular-dynamics calculations and technical details of the comparison of the theory with experiment are discussed in Sec. III. Section IV discusses the results. Our conclusions are summarized in Sec. V.

II. POTENTIAL FUNCTIONS

There are two types of interatomic potential functions used in molecular-dynamics calculations, *ab initio*

 ©1987 The American Physical Society

quantum-mechanical potentials and empirical potentials. *Ab initio* potentials are obtained by fitting a functional form to the results of quantum-mechanical calculations of the total energy of a collection of atoms as a function of their nuclear positions. Such potentials have been used for more than a decade for molecular-dynamics calculations of liquids containing small molecules and ions, but accurate *ab initio* potentials suitable for covalently bonded materials like germanium have not been developed. Empirical potentials are obtained by assuming a functional form that describes the physical features believed to be important in the correct potential and then obtaining values for the parameters in the function by using experimental data. In the present work, we use empirical potentials.

In any binary alloy there are three types of interactions to be considered. In the system of Mo-Ge they are (1) interactions among Ge atoms; (2) interactions among Mo atoms; and (3) interactions between Ge atoms and Mo atoms.

In principle, these interactions among atoms in a condensed phase might depend not only on the positions of the atoms but also on the density and composition of the material. This is commonly expected for metallic materials, in which an important contribution to the interatomic interaction comes from the interactions of the atomic cores with the conduction electrons. However, the experimental information available is not sufficient to determine the potentials completely if we allowed the empirical potentials to depend on composition and density, especially in the absence of a theoretical model for such a dependence. We therefore adopt, as a working hypothesis, the assumption that the part of the potential that determines the structure of these materials is independent of density and composition. This then gives a smaller number of interactions to be extracted from the data and our object is to see if a physically reasonable set of potential functions can be obtained that reproduces the structural features observed in the condensed phases of Mo, Ge, and their alloys. Also since we are primarily interested in the structures of the materials, rather than their thermodynamic and elastic properties, we ignore the volume dependent contribution to the energy of metallic materials caused by the conduction electrons, since at a given volume they have no effect on the arrangement of the atoms. Our hope is that the structure-determining interactions are sufficiently insensitive to density and composition that this scheme will be successful.

We have previously developed empirical potential functions for condensed phases of pure germanium.[5] They are of the type developed by Stillinger and Weber[6] for silicon, and they consist of short-ranged two-body and three-body interactions. The two-body potential has a single minimum representing the tendency for germanium atoms to form chemical bonds with each other. The three-body potential promotes the formation of 109° bond angles between the various bonds made by a germanium atom. This stabilizes the diamond-lattice crystal structure. It also inhibits the formation of more than four chemical bonds by an atom, since bonding to more than four atoms necessarily leads to some bond angles differing significantly from 109°. The parameters of the potential were chosen to fit experimental data on crystalline and amorphous germanium, including the density, cohesive energy, and elastic constants of the crystal and the radial distribution function of the amorphous solid obtained from the x-ray scattering experiments. These potentials for germanium were used in the present work on alloys. The functional forms and parameters are given in the Appendix.

Empirical potentials for interactions among molybdenum atoms have been proposed by van Heugten[7] and by Miller.[8] Both are pairwise additive two-body interactions. The former was obtained from analysis of phonon dispersion curves for crystalline molybdenum, and the latter was obtained from elastic constants and the vacancy formation energy. We rejected the van Heugten potential because, at the experimental density of crystalline molybdenum, it predicts a lower energy for the face-centered-cubic crystal structure than for the body-centered-cubic structure, whereas the experimental crystal structure is bcc. The Miller potential does give a lower energy for the bcc structure at the experimental crystal density, but preliminary calculations that used it to model the molybdenum-rich amorphous phases gave radial distribution functions in significant disagreement with experiment. In particular, for 65 at. % Mo, the split second peak in the experimental RDF is not reproduced and the height of the first peak is significantly lower than the experimental result. This suggests that the potential is not sufficiently repulsive for distances less than the location of the first minimum. To obtain a more repulsive potential, we multiplied the Miller potential by a factor of 3.5 and were able to get very satisfactory calculated structures for the molybdenum-rich alloys. This rescaled Miller potential is given in the Appendix and was used in all the calculations presented here. It shares a desirable feature of the original Miller potential in that it correctly predicts that the lowest-energy structure for crystalline molybdenum at the experimental density is bcc.

For interactions among Mo and Ge atoms, we at first chose two-body potentials of the Stillinger-Weber type, which allow the formation of a chemical bond between the metal and metalloid. The important parameters of the potential are the depth of the minimum of the potential and the distance at which the minimum occurs. The crystal structure of Mo_3Ge is known.[9] We performed lattice energy calculations for this crystal structure using our Mo-Mo two-body interaction, our Ge-Ge two-body and three-body interactions, and various choices of the Mo-Ge two-body interaction. We determined what values of the depth and location of the minimum in the Mo-Ge interaction are consistent with having the known crystal structure be a local minimum energy structure for a crystal. The range of acceptable values for the depth was quite large, but the acceptable values for the location of the minimum were restricted to a range between 2.57 and 2.82 Å. The choices that satisfied this test were further tested by performing molecular-dynamics calculations on amorphous alloys over a wide range of Mo concentration (2–65 %). However, despite extensive attempts using many different parameters for the Mo-Ge two-body in-

teraction, we could find no such potentials that were satisfactory in reproducing the experimental structure of these amorphous alloys.

Figure 1 shows a comparison of the structures of amorphous alloys obtained from experiment and from a typical calculation using only a two-body potential for the Mo-Ge interaction. The model fails to reproduce the qualitative features of the structural changes from the continuous random network of Ge at low Mo concentration to the dense random close packing at high Mo concentration. The deficiency is particularly serious for small Mo concentrations. A spurious third peak, centered at twice the Mo-Ge nearest-neighbor distance, develops too early as the MO concentration is increased. This observation suggests that for low MO concentrations a spurious close-packing pattern of Ge atoms has developed around Mo atoms, strongly distorting the continuous random network of Ge. Analysis of configurations confirmed this conjecture. The average Mo atom has a large number (12–13) of nearest-neighbor Ge atoms. More than half of the Ge atoms that are first neighbors of a Mo atom have five other Ge atoms surrounding them. The distorted structure that is produced has a radial distribution function very different from what is observed experimentally and an average coordination number that is higher than the experimental values for low Mo concentrations. Therefore, we abandoned the use of two-body potentials alone to describe the Mo-Ge interaction.

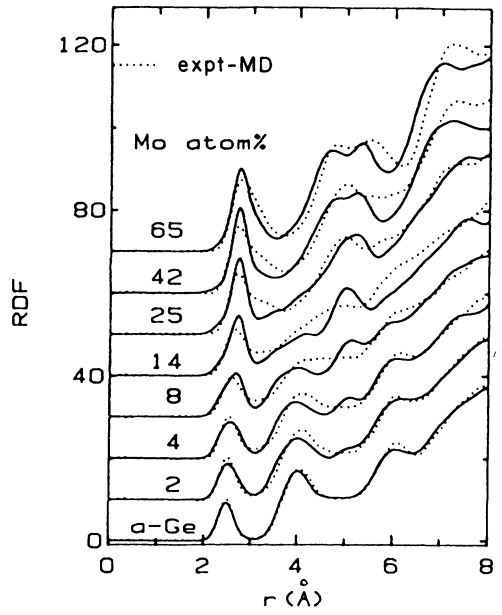

FIG. 1. Comparison of radial distribution functions obtained from a potential model with only a two-body potential for the Mo-Ge interaction (solid lines) and those from x-ray scattering experiments of Kortright and Bienenstock (dashed lines). The MD calculated results have been convolutionally broadened using Eq. (8) for a proper comparison with the experimental results. The parameters of the broadening are $a=0.01$ Å^2 and $k_{\max}=18.5$ Å^{-1}. All the curves are plotted on the same scale, but they are offset vertically. The significant discrepancies between the experimental results and many similar MD results led us to abandon the use of only two-body interactions for the Mo-Ge interaction.

A feature of the structure observed in these simulations is that a germanium atom that is a near-neighbor of a molybdenum atom also typically has four or five germanium neighbors. Germanium is expected to form at most four covalent bonds, and these four bonds should be in tetrahedral directions. If this tendency were strong enough, it would prevent the kind of close-packing coordination that we saw around molybdenum atoms. We suspected that this is the major physical element lacking in the potential model. One way to strengthen the tetrahedrality of the bonding of germanium atoms would be to include in the potential a three-body interaction that tends to establish a 109° angle between bonds made by a germanium to another germanium and to a molybdenum.[10] Thus we decided to use a three-body interaction of the Stillinger-Weber type is accomplish this.

The values of the parameters in this additional three-body potential were chosen by performing molecular-dynamics simulations of the amorphous alloys and seeing which sets of values led to structures in good agreement with experiment. The most important parameter is λ, which represents the overall strength of this three-body interaction. A value approximately half that for the three-body germanium interaction was finally chosen.

The final version of the potentials is given in the Appendix. All the results reported in this paper are associated with this set of potential functions, unless specified otherwise. They led to structures that are in very good agreement with the experimental data for the amorphous materials over the entire composition range studied. A detailed comparison of the theoretical and experimental structures is given below.

In Fig. 2 we plot the three pair potentials for the Mo-

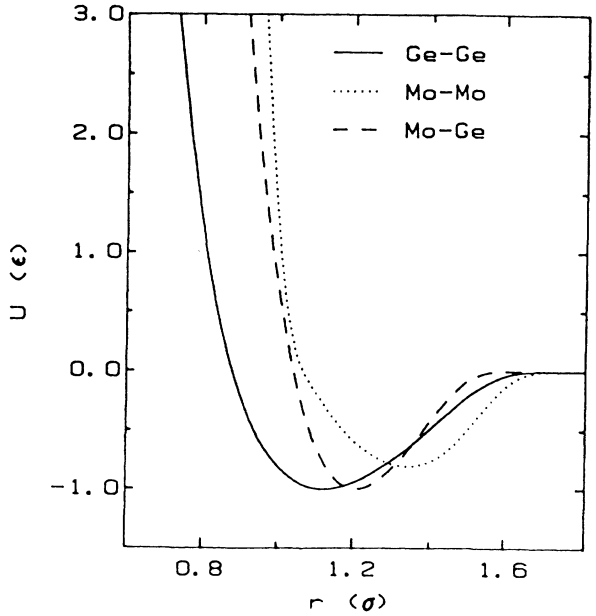

FIG. 2. Pair potentials for Mo-Mo [Eq. (A2)], Ge-Ge [Eq. (A1)], and Mo-Ge [Eq. (A1)] in reduced units. The unit of energy ϵ is 1.93 eV, and the reduced unit of length σ is 2.181 Å.

Mo, Ge-Ge, and Mo-Ge interactions. The relative depths of the three functions suggest that our model does not favor separation into pure Ge and pure Mo phases. The depth of the potential well for the Mo-Ge interaction ($E_{\min}=1.0\epsilon$) is larger than the average of the Mo-Mo and Ge-Ge interactions ($E_{\min}=0.81\epsilon$ and 1.0ϵ, respectively).

III. SOME TECHNICAL DETAILS OF THE CALCULATIONS

A. Molecular-dynamics calculations

The molecular-dynamics calculations performed in the current work used the velocity form of the Verlet algorithm[11] to integrate the classical equations of motion for a collection of 216–300 particles in a box of constant volume with periodic boundary conditions. The time step used in the numerical integration was 0.00136 psec, which is smaller than the reciprocal of the Debye frequency (on the order of 1–10 psec) of crystalline Ge.[12]

In a typical calculation, a system with the desired number of Mo and Ge particles and with the desired volume was thoroughly equilibrated for about 10000 time steps (or 14 psec) at a high temperature of about 4000 K, well above the melting temperature of molybdenum. The system volume was chosen so that the density of the system was equal to the experimental density of the amorphous alloy of the same composition. The system was then cooled from the liquid state to the amorphous solid state using the method of stochastic collisions (at random times particles were picked at random and their momenta were replaced by momenta chosen at random from a Boltzmann distribution at a low temperature). This process usually took about 10000–20000 time steps (or 14–27 psec), and it was immediately followed by annealing (for about 5000 time steps) at the final temperature, which is room temperature. Calculations of the radial distribution functions of the samples were then performed in a period of 5000 time steps. To test for system size effects, similar runs were also performed for samples of 400–500 atoms at various concentrations and the radial distribution functions were found to be in satisfactory agreement with those of the corresponding samples of smaller size.

B. RDF, PDF, DDF, and convolution broadening

The radial distribution functions we obtained from simulation were compared with x-ray and anomalous x-ray scattering results of Kortright and Bienenstock[1,2] for amorphous molybdenum-germanium alloys. In this section, we describe the connection between the experimental results they present and the theoretical results we calculate.

In x-ray scattering experiments, the observed intensity, in electron units, of the coherent scattering is related to the atomic structure in the following way:

$$I^{\rm coh}(q)=\left\langle \sum_j \sum_k f_j(q) f_k(q) \exp[-i\mathbf{q}\cdot(\mathbf{r}_j-\mathbf{r}_k)] \right\rangle . \quad (1)$$

Here the sums are over all atoms, and $\mathbf{r}_j$ and $f_j(q)$ denote the position and atomic scattering factor, respectively, of atom j. The scattering vector $\mathbf{q}$ has a magnitude of

$$q=|\mathbf{q}|=\frac{4\pi\sin\theta}{\lambda} , \quad (2)$$

where θ is half the scattering angle and λ is the wavelength of the x rays. The angular brackets denote a time average or ensemble average.

In principle, the atomic scattering factor $f_a(q)$ of an atom of type a depends on the photon energy E of the incident radiation, as well as the magnitude of the wave vector. It can be divided into an energy-independent part $f_a^0(q)$ and real and imaginary energy-dependent parts $f_a'(q,E)$ and $f_a''(q,E)$:

$$f_a(q,E)=f_a^0(q)+f_a'(q,E)+if_a''(q,E) . \quad (3)$$

The energy-independent part $f_a^0(q)$, is related to the Fourier transform of the electron density of the atom. It makes the major contribution to the $f_a(q,E)$ when the incident photon energy is far from the absorption edge of the a atom. The energy-dependent part, called the anomalous scattering factor, becomes significant only when photon energies are near absorption edges.

In the theory of liquids and in analyzing computer simulations, it is convenient to work with the pair-correlation functions $g_{ab}(r)$ defined so that $\rho_b g_{ab}(r)$ is the average microscopic density of b atoms a distance r away from an a atom. Here ρ_b denotes the average number density of b atoms in the sample. These correlation functions satisfy the symmetry property that $g_{ab}(r)=g_{ba}(r)$, and for an isotropic fluid or amorphous material they depend only on the scalar distance r and not on its vector direction.

The connection between the experimental coherent-scattering intensity $I^{\rm coh}$ and the theoretical pair-correlation functions can be made by defining the following partial structure factors:

$$S_{ab}(q)=\frac{4\pi\rho_b}{q}\int [g_{ab}(r)-1]r\sin(qr)dr . \quad (4)$$

It follows from these definitions that the coherent-scattering intensity for a two-component atomic material is given by

$$I^{\rm coh}(q)=w_{AA}(q)[S_{AA}(q)+1]+w_{AB}(q)S_{AB}(q) +w_{BB}(q)[S_{BB}(q)+1] , \quad (5)$$

where

$$w_{AA}(q)=x_A f_A^2(q) ,$$

$$w_{AB}(q)=2x_A \mathrm{Re}[f_A^*(q)f_B(q)] ,$$

and

$$w_{BB}(q)=x_B f_B^2(q) .$$

Here A and B refer to the two atomic species, and x_A and x_B are their atom fractions.

In principle, by performing scattering experiments at three different energies, three independent measurements of $I^{\rm coh}(q)$ would yield information on the three partial structure factors, which would then allow the three pair-correlation functions to be determined. In practice, this

procedure can not always be carried out because of the sensitivity of the results to small amounts of random and systematic error. Instead, the experimental data was presented as radial distribution functions (RDF's) and differential distribution function (DDF's), and only in favorable cases as partial distribution functions (PDF's).

The experimental RDF, as defined by Kortright and Bienenstock, is obtained in the following way. Experiments are performed for x-ray energies far from the absorption edges of the material. A total structure factor $S(q)$ is defined as

$$S(q)=\frac{[I^{\mathrm{coh}}(q)-\langle[f(q)]^2\rangle]}{\langle f(q)\rangle^2} , \tag{6}$$

where

$$\langle[f(q)]^2\rangle=x_A[f_A(q)]^2+x_B[f_B(q)]^2$$

and

$$\langle f(q)\rangle^2=[x_A f_A(q)+x_B f_B(q)]^2 .$$

The denominator in Eq. (6) approximately cancels the q dependence of the scattering factors in the numerator. [This follows from the assumption that the q dependence of the scattering factors of the two species are approximately the same, i.e.,

$$f_A(q)=Z_A F(q)$$

and

$$f_B(q)=Z_B F(q) ,$$

where the same $F(q)$ appears for both atomic species and $F(0)=1$.] $S(q)$ can be measured for a range of values of q. In the work of Kortright and Bienenstock it is multiplied by a Gaussian termination factor and the product is inverse Fourier transformed to give the experimental "radial distribution function" (RDF):

$$\mathcal{R}^{\mathrm{expt}}(r)=4\pi r^2\rho+\frac{2r}{\pi}\int_0^{k_m} qS(q) \times\exp(-aq^2)\sin(qr)dq , \tag{7}$$

where k_m is the experimental cutoff of q. If $S(q)$ could be obtained for all q and if no termination factors were used, $\mathcal{R}^{\mathrm{expt}}(r)$ would be simply equal to

$$\mathcal{R}(r)=\frac{4\pi\rho r^2[x_A^2 Z_A^2 g_{AA}(r)+2x_A x_B Z_A Z_B g_{AB}(r)+x_B^2 Z_B^2 g_{BB}(r)]}{(x_A Z_A+x_B Z_B)^2} .$$

Instead, $\mathcal{R}^{\mathrm{expt}}(r)$ is a convolution-broadened version of $\mathcal{R}(r)$. More precisely,

$$\mathcal{R}^{\mathrm{expt}}(R)=4\pi r^2\rho\left[1+\frac{2}{\pi r}\int r'[g(r')-1] \times G(k_m,a;r,r')dr'\right] , \tag{8}$$

where

$$g(r)=\frac{\mathcal{R}(r)}{4\pi r^2\rho}$$

and

$$G(k_m,a;r,r')=\int_0^{k_m}\exp(-ak^2)\sin(kr)\sin(kr')dk .$$

Thus, $\mathcal{R}^{\mathrm{expt}}(r)$ gives information about a weighted sum of all the three pair-correlation functions for a two-component system.

More detailed information about the structure is expressed by the differential structure factor (DSF) or differential distribution function (DDF) as defined by Kortright and Bienenstock. The experimental $\mathrm{DSF}_A^{\mathrm{expt}}$ is obtained by measuring the coherent scattering intensities both near and far from the absorption edge of atomic species A and subtracting the results. After normalization by a factor similar to the denominator of Eq. (6), which approximately cancels the q dependence of the scattering factors, and multiplication by a Gaussian termination factor, the result is Fourier transformed to r space to give the experimental "differential distribution function" for atomic species a. The idealized differential distribution function in the absence of convolution broadening is

$$\mathcal{D}_A(r)=4\pi r^2\rho\frac{[x_A Z_A g_{AA}(r)+x_B Z_B g_{AB}(r)]}{(x_A Z_A+x_B Z_B)} .$$

The experimental differential distribution function is related to the idealized DDF by a convolution broadening.

$$\mathcal{D}_A^{\mathrm{expt}}(r)=4\pi r^2\rho\left[1+\frac{2}{\pi r}\int r'[g_A(r)-1] \times G(k_m,a;r,r')dr'\right] , \tag{9}$$

where

$$g_A(r)=\frac{\mathcal{D}_A(r)}{4\pi r^2\rho} .$$

The DDF for species B is given by the formula above with A and B interchanged throughout. Thus each $\mathcal{D}^{\mathrm{expt}}$ gives information about a weighted sum of only two of the three pair-correlation functions for a two-component system.

In favorable situations, it is possible to perform three independent scattering experiments (one near the absorp-

TABLE I. Comparison of molecular-dynamics (MD) and experimental (Expt.) structural data for amorphous Mo-Ge alloys—properties of the RDF.

Mo (at. %)	r_1[a] MD	r_1[a] Expt.	r_1[a] Error[d]	$\mathcal{R}(r_1)$[b] MD	$\mathcal{R}(r_1)$[b] Expt.	$\mathcal{R}(r_1)$[b] Error[d]	CN[c] MD	CN[c] Expt.	CN[c] Error[d]
0	2.48	2.48	0.00	9.27	10.10	−8.22	4.01	4.00	0.25
2	2.52	2.50	0.80	8.51	10.20	−16.57	4.40	4.40	0.00
4	2.52	2.52	0.00	8.32	10.13	−17.87	4.70	4.80	−2.08
8	2.61	2.57	1.56	8.51	9.66	−11.90	5.40	5.20	3.85
14	2.71	2.64	2.65	11.60	11.20	3.57	6.30	6.00	5.00
25	2.74	2.70	1.48	13.40	14.60	−8.22	12.00	12.30	−2.44
42	2.76	2.72	1.47	17.10	15.90	7.55	12.00	12.40	−3.23
65	2.78	2.76	0.72	17.20	17.37	−0.98	13.10	13.50	−2.96

[a]Location of the first peak in the RDF in Å.
[b]$\mathcal{R}(r)$ is in units of atoms/Å. See Eq. (8) in the text.
[c]Nearest-neighbor coordination number, defined as the area of the first peak in the RDF, computed to a distance of 3.0 Å for samples of 0–14 at. % Mo and to a distance of 3.7 Å for higher concentrations of Mo.
[d]Percentage discrepancy between the MD and Expt. results.

tion edge of species A, one near that of B, and one far from both edges) and analyze the results to obtain one or more of the three structure factors S_{AA}, S_{AB}, and S_{BB}. The r space transform of the result can be used to construct experimental "partial distribution functions" $\mathcal{P}^{\text{expt}}$. The idealized PDF in the absence of convolution broadening is

$$\mathcal{P}_{ij}(4)=4\pi r^2\rho x_j g_{ij}(r) ,$$

where i and j each can be A or B. [There are nominally four such functions, but only three of them are independent since $\mathcal{P}_{AB}(r)$ and $\mathcal{P}_{BA}(r)$ are simple multiples of one another.] The experimental partial distribution functions are related to the idealized functions by a convolution broadening:

$$\mathcal{P}_{ij}^{\text{expt}}(r)=4\pi r^2\rho x_j \left[1+\frac{2}{\pi r}\int r'[g_{ij}(r')-1] \times G(k_m,a;r,r')dr'\right] . \quad (10)$$

In molecular-dynamics (MD) calculations, the pair-correlation functions $g_{AA}(r)$, $g_{AB}(r)$, and $g_{BB}(r)$ are calculated for $r<L/2$, where L is the length of the simulation box. To compare them with the experimental data, the results are convoluted according to Eqs. (8)–(10). (In performing the convolutions, we assume that the various pair-correlation functions are 1 for $r>L/2$. The calculated results for $r<L/2$ are not sensitive to the small errors in this assumption.) The resulted RDF, DDF's, and PDF's are then compared with the experimental results in r space for values of r less than $L/2$.

IV. RESULTS AND DISCUSSION

The results of molecular-dynamics calculations using the potentials described in Sec. II are given in Figs. 3–6 and in Tables I–IV, where they are compared with data of Kortright and Bienenstock obtained from x-ray scattering experiments. In many respects, the theoretical results are in excellent agreement with experiment. (1) The loca-

TABLE II. Comparison of molecular-dynamics (MD) and experimental (Expt.) structural data for amorphous Mo-Ge alloys—properties of the Ge DDF.

Mo (at. %)	r_1[a] MD	r_1[a] Expt.	r_1[a] Error[e]	$\mathcal{D}_{\text{Ge}}^{b}$ MD	$\mathcal{D}_{\text{Ge}}^{b}$ Expt.	$\mathcal{D}_{\text{Ge}}^{b}$ Error[e]	CN_{Ge}[c,d] MD	CN_{Ge}[c,d] Expt.	CN_{Ge}[c,d] Error[e]
14	2.67	2.67	0.00	9.67	11.02	5.85	5.80[c]	6.65[c]	−12.78
42	2.74	2.72	0.74	15.99	15.59	2.57	8.56[c]	9.00[c]	−4.89
							12.37[d]	13.70[d]	−9.68
65	2.71	2.72	−0.37	20.86	15.09	38.24	10.61[c]	9.50[c]	11.68
							13.97[d]	13.00[d]	7.46

[a]Location of the first peak in $\mathcal{D}_{\text{Ge}}$ in Å.
[b]$\mathcal{D}_{\text{Ge}}(r)$ in units of atoms/Å. See Eq. (9) in the text.
[c]Nearest-neighbor coordination number, defined as the area of the first peak of $\mathcal{D}_{\text{Ge}}$, computed to a distance of 3.0 Å.
[d]Nearest-neighbor coordination number, as defined in footnote c, computed to a distance of 3.7 Å.
[e]Percentage discrepancy between the MD and Expt. results.

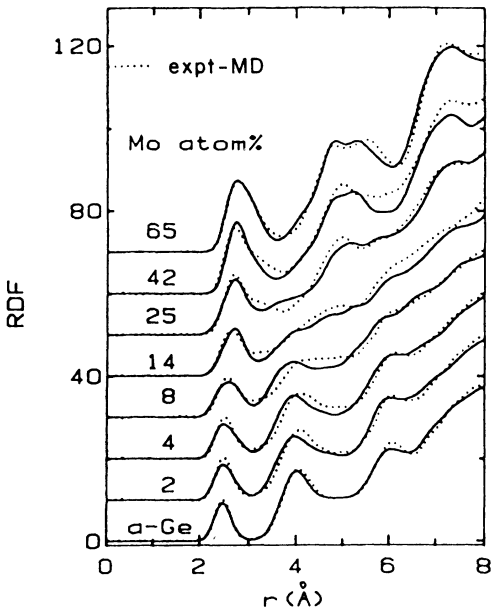

FIG. 3. Comparison of molecular-dynamics and experimental radial distribution functions of amorphous Mo-Ge alloys. Solid lines represent those from MD calculations and dashed lines those from x-ray scattering experiments of Kortright and Bienenstock. The MD results have been convolutionally broadened using Eq. (8) for a proper comparison with the experimental results. The parameters of the broadening are $a=0.01$ Å^2 and $k_{\max}=18.5$ Å^{-1}. All the curves are plotted on the same scale, but they are offset vertically.

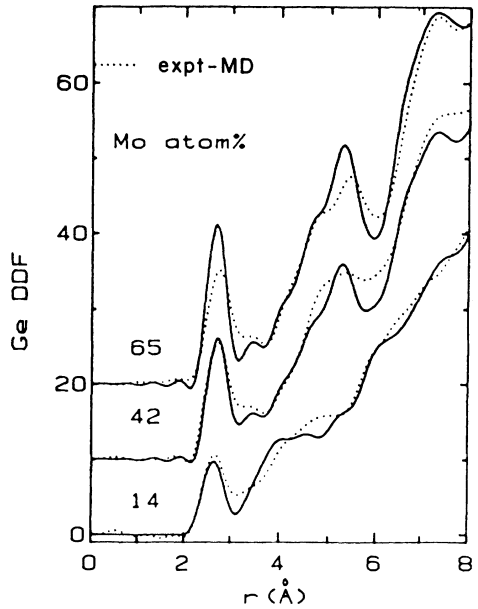

FIG. 4. Comparison of molecular-dynamics and experimental Ge differential distribution functions of amorphous Mo-Ge alloys at 14, 42, and 65 at. % Mo. Solid lines represent the $\mathcal{D}_{\mathrm{Ge}}$ from the MD simulation, and dashed lines are those from anomalous x-ray scattering experiments of Kortright and Bienenstock. The MD calculated results have been convolutionally broadened using Eq. (9) for a proper comparison with the experimental results. The parameters of the broadening are $a=0.01$ Å^2 and $k_{\max}=10.5$ Å^{-1}. All the curves are plotted on the same scale, but they are offset vertically.

tion of the first peak of the experimental RDF moves from 2.48–2.77 Å as the concentration of Mo is increased; a total change of about 11%. The corresponding MD first peak locations differ from the experimental values by at most 2.7%, with the average deviation being 1.4%. (2) The experimental coordination number (area under the first peak in the RDF) changes monotonically by a factor of 3.4, from 4.0 to 13.5, in going from pure Ge to the 65 at. % Mo alloy. The MD coordination numbers differ from the experimental ones by at most 5%. The average deviation is 2.5%. (3) The height of the first peak of the experimental RDF varies by a factor of 1.6 over this concentration range, while the MD height of the first peak is in error by at most 17%, with the average error being about 9%. (4) As the composition is changed, the overall shape of the experimental curves changes continuously from that of tetrahedral random network for pure a-Ge to that typical of the dense random close packing of spheres for the 65-at. % Mo alloy. This structural change is qualitatively well reproduced in the RDF curves obtained from molecular dynamics. All these observations strongly indicate that the short-range order is well described and the concentration dependence of the structures is well represented by the current potential model. The conclusions are also confirmed by the satisfactory agreement between the experimental and molecular-dynamics differential and partial distribution functions.

The agreement is not perfect, however. For example, there is a discrepancy between the MD calculations and experiment in some of the details around the first minimum and the second peak of the distribution functions. These deficiencies might be overcome by incorporating a three-body interaction involving Ge-Mo-Mo triplets, since the discrepancy occurs only for compositions at which both Mo-Mo and Mo-Ge pairs make comparable contributions to the radial distribution functions. Kortright[1] believes that Mo-Mo near neighbors with a long interatomic distance of 3.3 Å are responsible for the shoulders appearing in the experimental distribution functions at the large-r side of the first peak for samples with 14–42 at. % Mo. However, we have little intuition about what sorts of physically reasonable potentials would correct these deficiencies. Moreover, the deficiences are not expected to affect our structural interpretation of the materials in a significant way, since the amplitudes associated with them are rather small and since the calculated coordination numbers are in such good agreement with experiment.

With the potentials that achieve agreement between theory and experiment, the MD calculations further provide us with a detailed structural interpretation for the x-ray scattering data. Analysis of the configurations obtained from the MD calculations reveal that the Mo atoms tend to cluster together at low Mo concentrations. This is clearly seen from Fig. 7 where clusters formed by Mo atoms are plotted. This clustering of Mo atoms

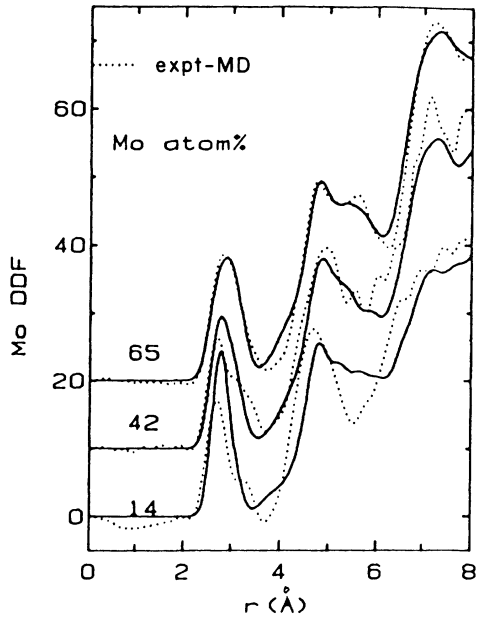

FIG. 5. Comparison of molecular-dynamics and experimental Mo differential distribution functions of amorphous Mo-Ge alloys at 14, 42, and 65 at. % Mo. Solid lines represent the $\mathcal{D}_{\mathrm{Mo}}$ from the MD calculations, and dashed lines are from anomalous x-ray scattering experiment by Kortright and Bienenstock. The MD calculated results have been convolutionally broadened using Eq. (9) for a proper comparison with the experimental results. The parameters of the broadening are $a=0.01$ Å^2 and $k_{\max}=18.5$ Å^{-1}. All the curves are plotted on the same scale, but they are offset vertically.

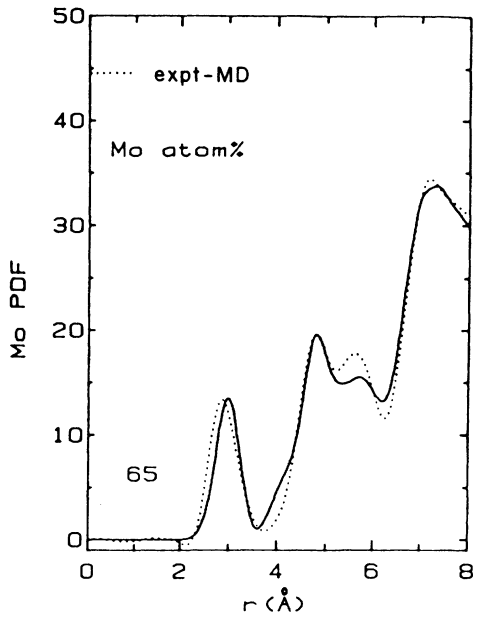

FIG. 6. Comparison of molecular dynamics and experimental Mo-Mo partial distribution functions $\mathcal{P}_{\mathrm{Mo\text{-}Mo}}$ for an amorphous Mo-Ge alloy with 65 at. % Mo. The solid line represents the MD result, and the dashed line is the experimental result of Kortright and Bienenstock. The MD calculated results have been convolutionally broadened using Eq. (10) for a proper comparison with the experimental results. The parameters of the broadening are $a=0.01$ Å^2 and $k_{\max}=18.5$ Å^{-1}.

occurs despite of the fact that in our model the Mo-Mo two-body interaction is less attractive than the Mo-Ge two-body interaction. These clusters are in the form of chains of Mo atoms that are occasionally branched and that can form rings. This clustering is in striking resemblance with the hydrophobic interaction in aqueous solutions, in which water forms a similar continuous tetrahedral random network and solutes that interact weakly with water tend to cluster together.

At low Mo concentrations, each molybdenum atom appears to be caged by Ge atoms. To study the coordination of Mo at low Mo concentration, we have performed simulations of samples containing a single Mo atom or a pair of Mo atoms that are constrained to be near neighbors. We found that there are, on average, about 10 Ge atoms in the first coordination shell of each Mo atom, very much like the situation in a Ge crystal when a Mo atom is interstitially incorporated into the diamond lattice of Ge. However, the presence of even one Mo atom does have some effect on the local chemical ordering around Ge atoms. In a configuration with one Mo atom, about 67% of the immediately neighboring Ge atoms are bonded to four other Ge atoms. About 24% of the nearest-neighbor Ge atoms are fivefold coordinated with other Ge atoms. Of the Ge atoms that are the second-nearest neighbors of the Mo atom, 76% are bonded to four other Ge atoms, and 22% to five. Similar bonding statistics are found in the configurations containing a bound Mo-Mo pair. When compared with the case in pure a-Ge, where 90% of Ge atoms are fourfold coordinated and 10% of them are fivefold coordinated, this observation strongly supports the idea that Mo atoms are not substitutionally incorporated into the RTN of Ge. Furthermore, it indicates that even a single-Mo atom or a pair of neighboring Mo atoms tend to modify significantly the RTN of Ge in its immediate vicinity while occupying interstitial-like holes in the network.

As more Mo atoms are added to the RTN of Ge, the influence of Mo atoms on the Ge network becomes stronger. The percentage of fourfold coordinated Ge atoms among the first- and second-nearest neighbors of Mo atoms decreases from greater than 65% to about

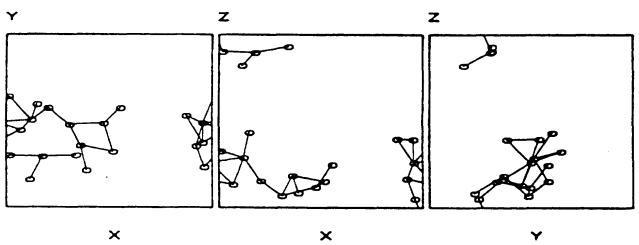

FIG. 7. Projections showing clustering of Mo atoms at 8 at. %. The three squares are views of the same configuration along Z, Y, and X axes. All Mo atoms are shown but not the Ge atoms. Lines are drawn between all pairs of Mo atoms that are nearest neighbors in the sense of being less than 3.05 Å apart.

TABLE III. Comparison of molecular-dynamics (MD) and experimental (Expt.) structural data for amorphous Mo-Ge alloys—properties of the Mo DDF.

Mo (at. %)	r_1[a] MD	r_1[a] Expt.	r_1[a] Error[e]	$\mathcal{D}^b_{Mo}$ MD	$\mathcal{D}^b_{Mo}$ Expt.	$\mathcal{D}^b_{Mo}$ Error[e]	CN_{Mo}[c,d] MD	CN_{Mo}[c,d] Expt.	CN_{Mo}[c,d] Error[e]
14	2.78	2.70	2.96	24.26	17.15	41.46	11.38[c]	8.60[c]	32.30
							13.20[d]	10.50[d]	25.71
42	2.80	2.70	3.70	19.34	16.50	17.21	10.83[c]	8.70[c]	24.43
							13.32[d]	12.70[d]	4.88
65	2.91	2.82	3.19	18.04	19.00	−5.05	13.99[d]	14.30[d]	−2.17

[a]Location of the first peak in $\mathcal{D}_{Mo}$ in Å.
[b]$\mathcal{D}_{Mo}$ in units of atoms/Å. See Eq. (9) in the text.
[c]Nearest-neighbor coordination number, defined as the area of the first peak of $\mathcal{D}_{Mo}$, computed to a distance of 3.0 Å.
[d]Nearest-neighbor coordination number, as defined in footnote c, computed to a distance of 3.7 Å.
[e]Percentage discrepancy between the MD and Expt. results.

50% to less than 35% when the concentration of Mo varies from less than 2% to 10% to greater than about 25%. Up to about 20 at. % Mo, the tetrahedral-like characteristics remain in the distribution of the bond angles made by two Ge–Ge bonds centered at Ge atoms that are the neighbors of Mo atoms. The Mo atoms cluster together and are no longer caged in the interstitial-like holes formed by Ge. This picture is much like that suggested by Kortright[1] that two distinct local structures, *a*-Ge-like and Mo-modified structures, coexist in region I on a very fine size scale. Analysis of the distribution of bond angles made by all Ge atoms indicates that the peak centered at $\sim 109°$ becomes essentially flat when the Mo concentration reaches 25%. This agrees with the analysis of Kortright and Bienenstock who concluded, on the basis of distribution functions, that tetrahedral *a*-Ge has disappeared by about 23 at. % Mo.

Kortright associated the Mo-modified structure with that of the Ge-rich intermetallic compound $MoGe_2$. The picture of the Mo-modified structure that emerges from the molecular-dynamics calculations has some similarities to, but also some differences from, the structure of crystalline $MoGe_2$. The important difference is that in $MoGe_2$ there are no molybdenum-molybdenum distances of less than about 3.5 Å, whereas the molecular-dynamics model of the amorphous material exhibits a clustering of the Mo atoms. A similarity between the crystal and the amorphous material is that the coordination number of Ge around Mo (out to a distance of 3.0 Å) is between 7.9 and 9.4 in the amorphous material and 9 in the crystal.

The clustering of Mo atoms at low Mo concentrations is remarkable since the two-body potential for the Mo-Mo interaction is the least attractive of the three two-body interactions and since the Mo-Ge attraction is stronger than the average of the Mo-Mo and Ge-Ge attractions. Some insight into the physical basis for the clustering can be obtained by comparing the structures obtained from different sets of potentials at the same composition. In particular, for 8 at. % Mo, we performed calculations for several different combinations of two- and three-body potentials in searching for the best potentials presented here, and some patterns emerged from the results. The two most important features of the potentials that were varied were the depth of the two-body Mo-Ge potential and the strength of the three-body Ge-Ge-Mo potential.

If the depth of the two-body Mo-Ge potential is varied, keeping the other features of the set of potentials unchanged, the result was to change the average composition of the nearest-neighbor shells of the two types of atoms in the direction that one would expect. Namely, an increase in the depth of the Mo-Ge interaction leads to an increase in the number of Mo-Ge nearest-neighbor pairs. This is accompanied however by a decrease in the number of Mo-Mo and Ge-Ge near-neighbor pairs, and the total coordination numbers of Mo and of Ge separately are not appreciably changed.

If the strength of the three-body Ge-Ge-Mo interaction is varied, the results are different. An increase in the strength of this three-body interaction leads to a decrease in the total coordination of Ge atoms, a decrease in the total coordination of Mo atoms, a decrease in the number of Mo-Ge near-neighbor pairs, an increase in the number of Mo-Mo near-neighbor pairs, and no change in the

TABLE IV. Comparison of molecular-dynamics (MD) and experimental (Expt.) structural data for amorphous Mo-Ge alloys—properties of the PDF.

Mo (at. %)	r_1[a] MD	r_1[a] Expt.	r_1[a] Error[c]	$\mathcal{P}_{Mo\text{-}Mo}$[b] MD	$\mathcal{P}_{Mo\text{-}Mo}$[b] Expt.	$\mathcal{P}_{Mo\text{-}Mo}$[b] Error[c]
65	3.02	2.87	5.23	13.40	14.00	−4.29

[a]Location of the first peak in PDF in Å.
[b]PDF in units of atoms/Å. See Eq. (10) in the text.
[c]Percentage discrepancy between the MD and Expt. results.

number of Ge-Ge near-neighbor pairs (corresponding to an average of 4 Ge atoms in the first coordination shell of Ge atoms).

The latter results can be interpreted simply in the following way. The three-body Ge-Ge-Mo interaction tends to inhibit a high coordination of Ge around Mo. In particular, configurations in which two Ge atoms and one Mo atom are all near neighbors of one another (which are common at high density in the absence of the three-body Ge-Ge-Mo interaction) are unfavored because the Ge-Ge-Mo bond angles would be significantly less than 109°. Hence, turning up this interaction will move some Ge atoms out of the first coordination shell of Mo. This will leave room for additional Mo atoms in the first coordination shell of Mo atoms, and in the high-density environment it is favorable for additional Mo-Mo near-neighbor pairs to form. Even after this happens, however, the total coordination number of Mo atoms is significantly less than the values in the absence of the Ge-Ge-Mo three-body interaction.

In other words, in a material that has a low Mo atom fraction, the Ge-Ge-Mo three-body interaction promotes a coordination number of Ge about Mo that is significantly less than 12. The two- and three-body germanium interactions promote a coordination number of Ge about Ge that is 4, corresponding to the tetrahedral random network. If the Mo atoms were randomly distributed in the material, the overall coordination number would be too low to fill the space efficiently (in effect, the entropy associated with this way of filling space would be too low). By having the Mo atoms cluster together, some of the entropy associated with the randomness of the Mo atom positions is lost, but the resulting higher average coordination number leads to a more efficient filling of space, giving a net higher entropy to the material. This interpretation of an entropy-driven clustering bears strong resemblance to the usual interpretations of hydrophobic interactions of nonpolar solutes in aqueous solution.

V. CONCLUSIONS

A potential model for amorphous molybdenum-germaniums alloys has been developed using molecular-dynamics computer simulations. The potential model has five ingredients; a set of three two-body potentials for the Mo-Mo, Ge-Ge, and Mo-Ge interactions and a set of two three-body interactions for the triplets of Ge-Ge-Ge and Ge-Ge-Mo. The major features of the experimental x-ray distribution functions are well reproduced by molecular-dynamics calculations using these potentials. The only major discrepancy between the MD calculations and experiment is in some of the details of the first valley and the second peak of the RDF. Part of these deficiencies might be overcome by incorporating a three-body interactions involving triplets of Ge-Mo-Mo.

The simulation also indicates that, at low concentrations of molybdenum in germanium, the Mo atom is an interstitial in the continuous random network formed by germanium. As the Mo concentration is increased, the molecular-dynamics model predicts that the Mo atoms tend to cluster together forming chains, branched chains, and rings of metal atoms embedded in a matrix of Ge atoms, whose structure is strongly influenced by the metal atoms.

The results of the molecular-dynamics calculations are a detailed structural model of amorphous molybdenum-germanium alloys as a function of composition. We have performed tight-binding electronic structure calculations on these structures to shed some light on the concentration dependence of the electrical properties of these materials, in particular the metal-insulator transition obtained at about 10% molybdenum. The results will be published in a separate report.[13]

TABLE V. Parameters for the Ge-Ge and Ge-Mo two-body potentials [see Eq. (A1)], in reduced units, ($\epsilon = 1.93$ eV, $\sigma = 2.181$ Å.)

	Ge-Ge	Mo-Ge
p	4	4
q	0	0
a	1.8	1.8
A	7.049 556 277	10.016 22
B	0.602 224 5584	0.978 233 1

ACKNOWLEDGMENTS

We are indebted to Professor A. Bienenstock and Dr. J. Kortright for sending us their experimental data prior to

TABLE VI. Parameters appearing in the modified Miller two-body potential [see Eq. (A2)] in reduced units.

i	r_i	a_i	b_i	c_i	d_i
1	0.719 853 3	−3 103.774	7 214.745	−5 772.685	1 617.969
2	0.791 838 6	1 985.137	−4 874.044	3 799.685	− 908.621 9
3	0.935 809 2	−1 587.658	5 184.394	−5 613.094	2 027.567
4	1.079 780	3.081 885	−0.945 609 6	−14.069 16	12.328 55
5	1.475 699	−79.652 73	365.328 7	−554.579 8	278.205 6
6	1.583 677	−12.877 45	48.077 14	−52.155 78	12.979 80
7	1.655 663	73.556 69	−381.240 2	658.648 8	−379.304 4
8	1.727 648	0	0	0	0

TABLE VII. Distances r_{min} in Å and depths E_{min} in eV of the minima in the two-body potentials

	Ge-Ge	Ge-Mo	Mo-Mo
r_{min}	2.45	2.63	2.93
E_{min}	1.93	1.93	0.81

TABLE VIII. Parameters in the Ge-Ge-Ge and Ge-Ge-Mo three-body interactions [see Eq. (A3)] in reduced units.

	Ge-Ge-Ge	Ge-Ge-Mo
λ	31	16
γ	1.2	1.2
a	1.8	1.8

publication and for numerous helpful discussions, and to Professor T. H. Geballe and Professor W. A. Harrison for stimulating and rewarding communications. This work was supported by the National Science Foundation (under Grant No.-CHE84-10701) and by the Stanford University Center for Materials Research (funded by the National Science Foundation.)

APPENDIX: EMPIRICAL POTENTIALS FOR MoGe ALLOYS

The Ge-Ge and Ge-Mo two-body interactions are described by two-body functions of the type proposed by Stillinger and Weber:[6]

$$u_2(r_{ij})=\begin{cases} A\,(Br^{-p}-r^{-q})\exp[(r_{ij}-a)^{-1}], & r<a \\ 0, & r>a\ . \end{cases} \tag{A1}$$

The parameters, in reduced units ($\epsilon=1.93$ eV and $\sigma=2.181$ Å), are given in Table V.

The Mo-Mo two-body potential is a modification of that of Miller.[8] It is given by

$$u_2(r)=\begin{cases} c\exp(-dr), & 0<r<r_0 \\ a_ir^3+b_ir^2+c_ir+d_i, & r_i<r<r_{i+1},\ i=1,7 \\ 0, & r>r_8\ , \end{cases} \tag{A2}$$

with $c=1\,434.220$ and $d=4.861\,989$. The parameters associated with the polynomial functions are given in Table VI. The parameters are in reduced units.

Each of three potentials has a single minimum. These potentials are shown in Fig. 2. The locations of the minima and their depths are given in Table VII.

The three-body Ge-Ge-Ge and Ge-Ge-Mo interactions are described by three-body functions of the type proposed by Stillinger and Weber. In the Ge-Ge-Ge interaction, for each triplet of germanium atoms such that one atom (call it atom 1) is less than a certain cut-off distance a from two other atoms (call them 2 and 3), there is a contribution to the energy of the form:

$$u_3(r,s,t)=\lambda\exp[\gamma(r-a)^{-1}+\gamma(s-a)^{-1}](\cos\theta+\tfrac{1}{3})^2\ , \tag{A3}$$

where

$$\cos\theta=(r^2+s^2-t^2)/2rs\ .$$

The values of the parameters in reduced units are given in Table VIII. Here r is the scalar distance between atoms 1 and 2, s is the distance between atoms and 1 and 3, and t is the distance between atoms 2 and 3. For each atom 1 and each unordered pair of atoms 2 and 3, there is one such contribution, provided 1 is within a distance a of both 2 and 3. (Note that when all three atoms are within a distance a of each other, there will be three such separate contributions, with each of the three atoms playing the role of atom 1.) In the Ge-Ge-Mo three-body interaction, for each pair of germanium atoms (call them 1 and 2) and each Mo atom (call it 3) such that atom 1 is less than a cut-off distance a from both atoms 2 and 3, there is a contribution to the energy of the same form as given above, with parameters given in Table VIII. For each ordered triplet of atoms, 1, 2, and 3, there is one such contribution, provided 1 is within a distance a of 2 and of 3 and provided 1 and 2 are Ge atoms and 3 is an Mo atom. (Note that when all three atoms are within a distance a of each other, there will be two such separate contributions, with each of the Ge atoms playing the role of atom 1.)

Unless otherwise noted, all molecular-dynamics results in this paper were obtained with this set of potentials. The Ge-Ge two-body interaction and the Ge-Ge-Ge three-body interaction are the same as those used in previous work on amorphous germanium.[5]

[1]J. B. Kortright, Ph. D. thesis, Department of Materials Science and Engineering, Stanford University, 1984; also, Stanford Synchrotron Radiation Laboratory Report No. 84/05 (unpublished).

[2]J. B. Kortright and A. Bienenstock (unpublished).

[3]S. Yoshizumi, D. Mael, T. H. Geballe, and R. L. Greene, in *Localization and Metal-Insulator Transitions*, edited by H. Fritzsche and D. Adler (Plenum, New York, 1985), pp. 77–87.

[4]S. Yoshizumi, Ph.D. thesis, Department of Materials Science and Engineering, Stanford University, 1986; also, Edward L. Ginzton Laboratory Report No. 4020, Stanford University (unpublished).

[5]K. Ding and H. C. Andersen, Phys. Rev. B **34**, 6987 (1986).

[6]F. H. Stillinger and T. A. Weber, Phys. Rev. B **31**, 5262 (1985).

[7]W. F. W. M. van Heutgen, Phys. Status Solidi B **82**, 501 (1977).

[8]K. M. Miller, J. Phys. F **11**, 1175 (1981).

[9]*Atomic Energy Review Special Issue No. 7—Molybdenum: Physico-chemical Properties of its Compounds and Alloys,* edited by L. Brewer (International Atomic Energy Agency, Vienna, 1980), and references therein.

[10]This suggests that a three-body interaction that tends to establish a 109° angle between bonds made by a germanium to two molybdenum atoms might be required, as well. Such a three-body interaction appears not to be as important as the three-body potentials we retained, since, without it, we found a good agreement with the experiment at high-Mo concentration. We did not include this complication because we were trying to find the simplest interactions that can rationalize the experimental structures.

[11]W. C. Swope, H. C. Andersen, P. H. Berens, and K. R. Wilson, J. Chem. Phys. **76**, 637 (1982).

[12]K. A. Schneider Jr., *Solid State Physics,* edited by H. Ehrenreich, F. Seitz, and D. Turnbull (Academic, New York, 1964), Vol. 16, p. 368.

[13]K. Ding and H. C. Andersen, following paper, Phys. Rev. B **36**, 2687 (1987).